Ultralow-light-level all-optical transistor in rubidium vapor

Cite as: Appl. Phys. Lett. **104**, 151103 (2014); https://doi.org/10.1063/1.4871384
Submitted: 26 November 2013 • Accepted: 03 April 2014 • Published Online: 14 April 2014

Jietai Jing, Zhifan Zhou, Cunjin Liu, et al.

Ultralow-light-level all-optical transistor in rubidium vapor

Jietai Jing,[1,2,a)] Zhifan Zhou,[1,2] Cunjin Liu,[1,2] Zhongzhong Qin,[1,2] Yami Fang,[1,2] Jun Zhou,[1,2] and Weiping Zhang[1,2]
[1]*State Key Laboratory of Precision Spectroscopy, Department of Physics, East China Normal University, Shanghai 200062, People's Republic of China*
[2]*Department of Physics, Quantum Institute for Light and Atoms, East China Normal University, Shanghai 200062, People's Republic of China*

(Received 26 November 2013; accepted 3 April 2014; published online 14 April 2014)

An all-optical transistor (AOT) is a device in which one light beam can efficiently manipulate another. It is the foundational component of an all-optical communication network. An AOT that can operate at ultralow light levels is especially attractive for its potential application in the quantum information field. Here, we demonstrate an AOT driven by a weak light beam with an energy density of 2.5×10^{-5} photons/$(\lambda^2/2\pi)$ (corresponding to 6 yJ/$(\lambda^2/2\pi)$ and about 800 total photons) using the double-Λ four-wave mixing process in hot rubidium vapor. This makes it a promising candidate for ultralow-light-level optical communication and quantum information science. © *2014 AIP Publishing LLC*. [http://dx.doi.org/10.1063/1.4871384]

All-optical devices,[1–5] especially those operating in the ultralow light regime or even in the single-photon regime have attracted enormous attention in the field of all-optical communication and quantum information science. Photons are good candidates to be information carriers due to their strong immunity against decoherence.[6–8] Normally, the strength of the interaction between weak light beams and matter is quite small. It requires a large optical nonlinearity and long interaction time to achieve strong interaction. Currently, there are several means to realize low-light-level all-optical devices, such as approaches based on electromagnetically induced transparency,[9,10] cavity quantum electrodynamics,[5,11–14] optomechanically induced transparency,[15] and parametric down conversion.[16] In addition, conical emission (CE), which is one example of transverse pattern formation in nonlinear systems,[17] is a desirable alternative choice in the field of low-light-level all-optical devices for the advantage of simple setup and convenient manipulation.[18]

The four-wave mixing (FWM) process in a double-Λ system has been demonstrated as a valid way to provide strong dispersion of the index of refraction, which will further reduce the group velocity of the probe and thus enhance the interaction strength by prolonging the interaction time.[19–25] This is very critical for nonlinear optics at low light levels in the connection between ultraslow light propagation and strong light-matter interaction.[10,26,27] When the phase matching condition is fulfilled, an enhanced gain can be achieved in the double-Λ system. Here, we show that FWM in a double-Λ system leading to CE offers an alternative way to realize a cascade all-optical transistor (AOT) operating in the ultralow light regime.

The experiment is based on the FWM process in atoms with a double-Λ configuration (Figs. 1(a) and 1(b)). The laser beams used in the experiment are derived from a Ti:Sapphire laser which is locked to a stable temperature-controlled Fabry-Perot cavity located in a vacuum environment by the Pound-Drever-Hall technique. The output of this Ti:Sapphire laser is split into two parts, one of which is used as the pump beam with a power of about 400 mW and a beam waist of 2 mm. The other part of the laser is frequency-red-shifted about 3.03 GHz through an acousto-optic modulator to serve as the probe beam. With a beam waist of 1 mm and polarization orthogonal to the pump beam, the probe beam is injected at a small angle across the pump beam. The two beams are combined through a Glan-Laser polarizer which has an extinction ratio of more than 10^5:1 and sent into a hot rubidium vapor cell. The natural-abundance 7.5 cm rubidium vapor cell used in our experiment is wrapped by three layers of magnetic-shielding materials and heated by a resistive heater (outside of the magnetic-shielding) to 145 °C (corresponding to an atomic density of $\sim 3 \times 10^{13}$ atoms/cm^3). The Doppler-broadened line width of the resonant transition is about 590 MHz. The cell is tilted with respect to the incident beams to prevent the possible oscillation between the uncoated windows, which is also served as the means to introduce the slight asymmetry for building up the double-spot pattern. By setting the pump laser frequency at about 1.3 GHz blue detuned from the optical transition connecting the F = 2 ground state to the $F' = (2, 3)$ excited states of the D1 line of ^{85}Rb at 795 nm, a bright CE can be observed in the far field under perfectly symmetric conditions (Fig. 1(c)). The induced CE is projected onto a screen in the far field and is recorded by a camera. The probe beam and the pump beam are crossed at the center of the vapor cell with a small angle which equals to the cone half-angle of the CE. The second Glan-Laser polarizer is used to filter out the residual pump beam, which ensures the high visibility of the transverse patterns. The measured cone half-angle is about 8 mrad which is determined by the phase matching condition. With the symmetry breaking introduced by the slight tilt of the cell, the cone collapses into a bright double-spot pattern with a much weaker ring background (Fig. 1(d)). Allowing the probe beam to propagate along the conical surface, but at a different azimuthal angle will cause the double-spot pattern to rotate according to the direction of the probe beam (Fig. 1(e)).

[a)]Author to whom correspondence should be addressed. Electronic mail: jtjing@phy.ecnu.edu.cn

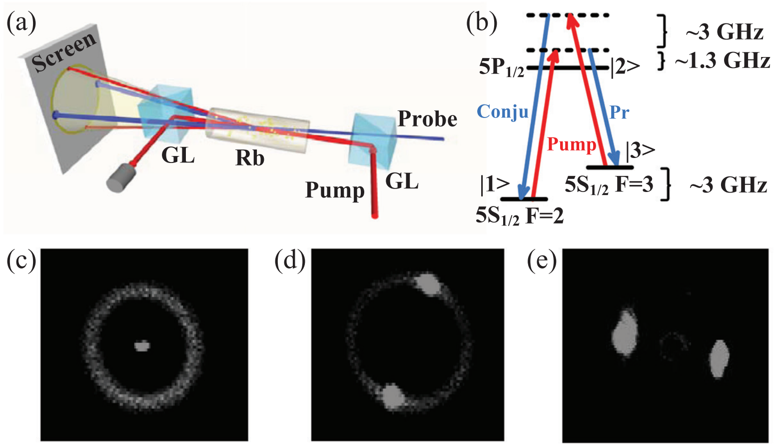

FIG. 1. Experiment. (a) Experimental layout. Rb, Rubidium vapor; GL, Glan-Laser polarizer. (b) The energy level diagram for the FWM process in the D1 line of ^{85}Rb. Pr, probe beam; Conju, conjugate beam. The $|1\rangle$ and $|3\rangle$ represent the ground states of $5S_{1/2}$, F = 2 and $5S_{1/2}$, F = 3, $|2\rangle$ indicates the $F' = (2, 3)$ excited states of the D1 line of ^{85}Rb. The pump beam is about 1.3 GHz blue detuned to the optical transition between $|1\rangle$ and $|2\rangle$ states. The broadening of $|2\rangle$ is meant to suggest the presence of several hyperfine levels as well as Doppler broadening of the transition. (c) The CE pattern is derived with good experimental setup symmetry. (d) The double-spot pattern with slight symmetry breaking in the setup. (e) Stimulated double-spot pattern which is significantly amplified and rotated to the direction of the probe beam.

Accompanying this switching effect, the probe beam gets amplified while a bright conjugate beam is generated on the opposite side of the pump.

The gain feature of this FWM process is characterized by plotting the measured probe (black) and conjugate (red) beam total power as a function of the two-photon detuning in Fig. 2, where red curves indicate the Gaussian profile fit of conjugate beam power data (red circles), and black curves indicate the Gaussian profile fit of probe beam power data (black squares). In Fig. 2(a), the full width at half maximum (FWHM) is found to be ~1.9 MHz for a probe beam power P = 180 pW; In Fig. 2(b), the FWHM is ~2.3 MHz for a probe beam power P = 2.8 nW; In Fig. 2(c), the FWHM is ~2.6 MHz for a probe beam power P = 33 nW. The consistent background is due to the residual spontaneous CE background. Optimal FWM gain requires a perfect phase matching condition which can be adjusted by a small change of the two-photon detuning.[20] The obtained sharp gain feature leads to a steep dispersion within the small frequency range (FWHM is ~1–3 MHz depending on the probe beam power) and results in a huge group velocity reduction.

The measured slow probe and conjugate pulses are shown in Fig. 3. The probe pulse with 500 ns FWHM is delayed by ~585 ns. During this process, a matched pulse with similar profile and a delay of ~510 ns is generated on the opposite side of the pump. The relative delay between probe and conjugate beams is a fundamental property of the dynamics of the system. These results indicate fractional delay, which is defined by the ratio of the delay to the pulse FWHM. A fractional delay of larger than unity is achieved here with only modest pulse broadening. The slow light effect can significantly extend the interaction time and further enhance the interaction strength of the light with the atomic ensemble. This ensures the possibility of this system operating at the low light level.

Based on the capability of the weak probe beam to manipulate the generated transverse pattern power, a cascade AOT operated in low light regime can be realized. As depicted in Fig. 4(a), ~180 pW power of probe beam induces generation of ~0.9 mW power of the output probe beam and ~1.2 mW of the conjugate beam, which provides a gain of ~5.0×10^6. As the probe beam power increases, the output pattern power also increases. Until the probe beam reaches ~50 μW, the output probe beam power is saturated at ~10 mW, and the conjugate beam power is saturated at ~20 mW. The different power level between the probe and conjugate beams is due to the fact that the probe beam's frequency is within the Doppler profile and then subject to the absorption, while the conjugate beam is far away from resonance and the absorption is negligible. The results shown in

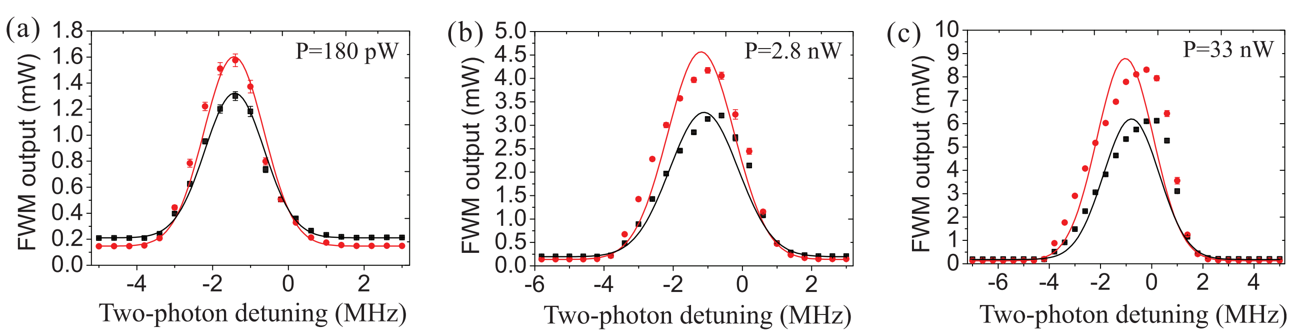

FIG. 2. Two-photon detuning effect. (a) The FWHM is ~1.9 MHz with 180 pW probe beam power; (b) The FWHM is ~2.3 MHz with 2.8 nW probe beam power; (c) The FWHM is ~2.6 MHz with 33 nW probe beam power. Error bars shown are ±s.d.

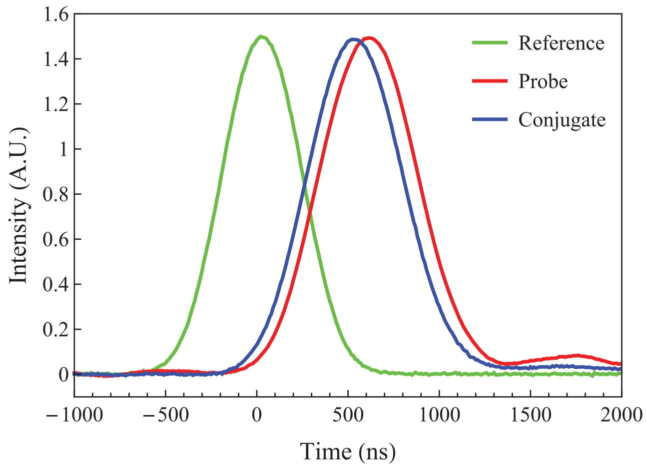

FIG. 3. Slow propagations of the probe and conjugate beams. The huge gain feature existing in this FWM process sharply changes the index of refraction as a function of frequency; this significantly reduces the group velocity of the probe beam (red solid curve). In this process, the conjugate beam (blue solid curve) is generated and propagates through the vapor cell on the other side of the pump. The green pulse is the reference signal used in the experiment without passing through the vapor cell. The probe and conjugate pulses are delayed by ~585 ns and ~510 ns, respectively. The ~500 ns delay corresponds to the group velocity of ~c/2000.

Fig. 4(a) indicate the AOT's functions of amplification and saturation, which is similar to the electronic transistor.

In addition to the amplification function described above, all-optical switching effect can also be observed in this system. As depicted in Fig. 4(b) top, with ~180 pW probe beam power, a switching efficiency of ~50% can be obtained for the spontaneous double-spot pattern in which each spot has a power of ~1 mW. The rising time of the switch is ~980 ns (Fig. 4(d)), which corresponds to ~800 photons needed to change its state. Energy density E, given in units of photons/$(\lambda^2/2\pi)$, is another metric to characterize the low light level all-optical switching. For the spot size of the probe beam (~1 mm beam waist) used in our experiment, the energy density is 2.5×10^{-5} photons/$(\lambda^2/2\pi)$, corresponding to 6 yJ/$(\lambda^2/2\pi)$. When the probe beam's power rises up to 2.8 nW, a switching efficiency of 90% can be achieved (Fig. 4(c) top) with ~625 ns rise-time (Fig. 4(e)), which represents ~7000 photons and 2.2×10^{-4} photons/$(\lambda^2/2\pi)$ (56 yJ/$(\lambda^2/2\pi)$) energy density. The spontaneous double-spot pattern switching efficiency and the rise-time depend on the probe beam power. The stronger the probe beam, the higher switching efficiency, and the shorter rise-time. The switching efficiency can reach almost unity once a ~30 nw probe beam is injected. At a power level above several μW, the rise-time is saturated at about 300 ns.

For comparison, the amount of amplification (~5.0×10^6) in this system far exceeds those demonstrated by other configurations. A gain of 30 in rubidium vapor using 280 mW of pump power off-resonance from all transitions was realized.[23] FWM in sodium vapor was used to observe a gain of 55 with response times of ~1 μs.[22] An efficient FWM with gains greater than 100 in Rb vapor confined to a hollow-core photonic band-gap fiber was also shown.[28] The scheme of mirrorless parametric self-oscillation in a rubidium vapor could provide a gain of 6500.[18]

It must be pointed out that our experiment is different from the previous work of Gauthier's group at Duke University.[18] First of all, although the phenomenon of CE has been experimentally demonstrated in a wide variety of atomic systems,[17] many of these patterns employ some sort of feedback effect via a single feedback mirror, the laser beams counter-propagating through an atomic vapor,[18] or utilizing of the cavity. However, the CE observed in our system occurs in a single pass medium without feedback. The pattern is symmetric and its frequency component shows that the FWM has involved the ground states which make it convenient to use atomic coherence to enhance the interaction between atoms and optical fields.[19–26] Second, the energy diagram used in our system is a double-Λ configuration. Recently, it has been demonstrated that a similar configuration of FWM in a double-Λ system of

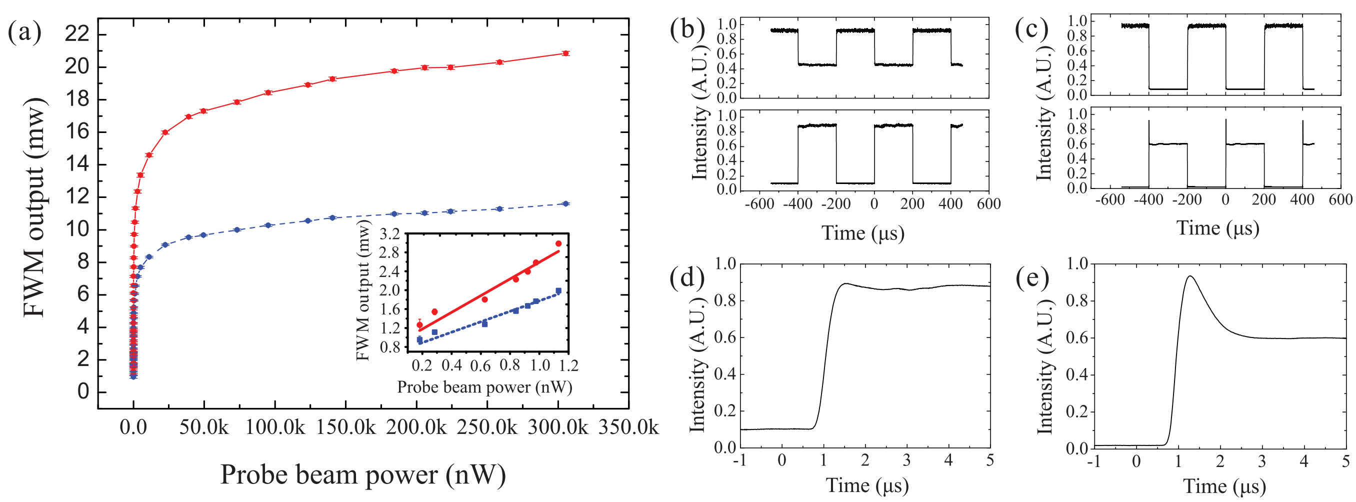

FIG. 4. AOT with amplification and switching functions. (a) The FWM signal versus probe beam power. The red solid curve is for the generated conjugate beam power (circles) and blue dashed curve is for the amplified probe beam power (squares). The inset shows the behaviour in the low light regime (the solid and dashed curves are linear fits of the data). Error bars shown are ±s.d. (b)–(e) Dynamical behaviours of the low light AOT. We pick up one spot of each spontaneous and stimulated double-spot pattern and send them into two photodiodes. (b) top and (c) top are the observed temporal evolutions of the spontaneous spot with 180 pW and 2.8 nW probe beam, respectively. 50% and 90% switching efficiency are achieved. (b) bottom and (c) bottom are the observed temporal evolutions of the stimulated spot with 180 pW and 2.8 nW probe beams, respectively. The rise-time of the stimulated spot is 980 ns for 180 pW (shown in (d)) and 645 ns for 2.8 nW (shown in (e)).

atomic vapor could be used as an efficient source to generate highly entangled beams and entangled quantum images.[29,30] The present scheme may be beneficial for exploring the entanglement properties potentially existing in this system. Thus, it is predictable an all-optical quantum device could be further developed which will integrate the abilities of generation, switching, delay, and amplification of entangled light beams.

We have experimentally demonstrated an AOT operating at ultralow light level based on the FWM process in a double-Λ system of a hot rubidium vapor cell. The steep gain feature results in slow propagation of the two matched pulses, which greatly enhances the nonlinear interaction at low light levels. The required probe beam power for maintaining a switching efficiency of 50% can be as low as 180 pW, and it can manipulate a light beam with power of 5.0×10^6 times more, which proves the cascade of the AOT. This AOT with ultralow light sensitivity and significant slow light effect may find application in all-optical quantum networks.[6–8] Further, improvements could include: adjusting the length of the vapor cell, or using a vapor cell with buffer gas. In this way, we believe that this AOT can be operated in the single-photon level and thus play an important role in the future quantum information and quantum communication field.[10–12]

We thank Professor Luis Orozco, Professor Paul Lett, and Professor G. Dong for fruitful discussions. This work was supported by the National Basic Research Program of China (973 Program) under Grant No. 2011CB921604, the National Natural Science Foundation of China under Grant Nos. 11374104, 10974057, and 11234003, the Shanghai Pujiang Program under Grant No. 09PJ1404400, the Program for Professor of Special Appointment (Eastern Scholar) at Shanghai Institutions of Higher Learning, the Program for New Century Excellent Talents in University (No. NCET-10-0383), the Shu Guang Project supported by Shanghai Municipal Education Commission and Shanghai Education Development Foundation (No. 11SG26), Specialized Research Fund for the Doctoral Program of Higher Education (20130076110011), and the Scientific Research Foundation for the Returned Overseas Chinese Scholars, State Education Ministry.

[1] D. A. B. Miller, Nat. Photonics **4**, 3–5 (2010).
[2] J. Hwang, M. Pototschnig, R. Lettow, G. Zumofen, A. Renn, S. Götzinger, and V. Sandoghdar, Nature **460**, 76–80 (2009).
[3] I. Fushman, D. Englund, A. Faraon, N. Stoltz, P. Petroff, and J. Vučković, Science **320**, 769–772 (2008).
[4] D. E. Chang, A. S. Sørensen, E. A. Demler, and M. D. Lukin, Nat. Phys. **3**, 807–812 (2007).
[5] W. Chen, K. M. Beck, R. Bücker, M. Gullans, M. D. Lukin, H. Tanji-Suzuki, and V. Vuletić, Science **341**, 768–770 (2013).
[6] L.-M. Duan, M. D. Lukin, J. I. Cirac, and P. Zoller, Nature **414**, 413–418 (2001).
[7] D. Bouwmeester, A. K. Ekert, and A. Zeilinger, *The Physics of Quantum Information* (Springer Press, 2000).
[8] H. J. Kimble, Nature **453**, 1023–1030 (2008).
[9] M. Bajcsy, S. Hofferberth, V. Balic, T. Peyronel, M. Hafezi, A. S. Zibrov, V. Vuletic, and M. D. Lukin, Phys. Rev. Lett. **102**, 203902 (2009).
[10] J. Zhang, G. Hernandez, and Y. Zhu, Opt. Lett. **32**, 1317–1319 (2007).
[11] M. Mücke, E. Figueroa, J. Bochmann, C. Hahn, K. Murr, S. Ritter, C. J. Villas-Boas, and G. Rempe, Nature **465**, 755–758 (2010).
[12] C. J. Hood, M. S. Chapman, T. Lynn, and H. J. Kimble, Phys. Rev. Lett. **80**, 4157–4160 (1998).
[13] K. M. Birnbaum, A. Boca, R. Miller, A. D. Boozer, T. E. Northup, and H. J. Kimble, Nature **436**, 87–90 (2005).
[14] K. Nozaki, T. Tanabe, A. Shinya, S. Matsuo, T. Sato, H. Taniyama, and M. Notomi, Nat. Photonics **4**, 477–483 (2010).
[15] S. Weis, R. Rivière, S. Deléglise, E. Gavartin, O. Arcizet, A. Schliesser, and T. J. Kippenberg, Science **330**, 1520–1523 (2010).
[16] K. J. Resch, J. S. Lundeen, and A. M. Steinberg, Phys. Rev. Lett. **89**, 037904 (2002).
[17] R. W. Boyd, S. G. Lukishova, and Y. R. Shen, *Self-Focusing: Past and Present* (Springer Press, 2009).
[18] A. M. C. Dawes, L. Illing, S. M. Clark, and D. J. Gauthier, Science **308**, 672–674 (2005).
[19] A. J. Merriam, S. J. Sharpe, M. Shverdin, D. Manuszak, G. Yin, and S. E. Harris, Phys. Rev. Lett. **84**, 5308–5311 (2000).
[20] M. D. Lukin, Rev. Mod. Phys. **75**, 457–472 (2003).
[21] M. D. Lukin, P. Hemmer, M. Löffler, and M. O. Scully, Phys. Rev. Lett. **81**, 2675–2678 (1998).
[22] P. R. Hemmer, D. P. Katz, J. Donoghue, M. Cronin-Golomb, M. S. Shahriar, and P. Kumar, Opt. Lett. **20**, 982–984 (1995).
[23] V. Boyer, C. F. McCormick, E. Arimondo, and P. D. Lett, Phys. Rev. Lett. **99**, 143601 (2007).
[24] A. M. Marino, R. C. Pooser, V. Boyer, and P. D. Lett, Nature **457**, 859–862 (2009).
[25] R. M. Camacho, P. K. Vudyasetu, and J. C. Howell, Nat. Photonics **3**, 103–106 (2009).
[26] M. M. Kash, V. A. Sautenkov, A. S. Zibrov, L. Hollberg, G. R. Welch, M. D. Lukin, Y. Rostovtsev, E. S. Fry, and M. O. Scully, Phys. Rev. Lett. **82**, 5229–5232 (1999).
[27] S. E. Harris and L. V. Hau, Phys. Rev. Lett. **82**, 4611–4614 (1999).
[28] P. Londero, V. Venkataraman, A. R. Bhagwat, A. D. Slepkov, and A. L. Gaeta, Phys. Rev. Lett. **103**, 043602 (2009).
[29] C. F. McCormick, V. Boyer, E. Arimondo, and P. D. Lett, Opt. Lett. **32**, 178–180 (2007).
[30] V. Boyer, A. M. Marino, R. C. Pooser, and P. D. Lett, Science **321**, 544–547 (2008).